Peer-reviewed version available at Biomimetics 2018, 3, 36; doi:10.3390/biomimetics3040036

Enzymatically active polydopamine @ alkaline phosphatase nanoparticles produced by $NaIO_4$ oxidation of dopamine.

Salima El Yakhlifi[1] , Dris Ihiawakrim [3], Ovidiu Ersen [3] and Vincent Ball [1,2]

1: Institut National de la Santé et de la Recherche Médicale

Unité Mixte de Recherche 1121.

11 rue Humann

67085 Strasbourg Cedex

2 : Université de Strasbourg

Faculté de Chirurgie Dentaire

8 rue Sainte Elisabeth

67000 Strasbourg

3: Institut de Physique et de Chimie des Matériaux.

UMR 7504 CNRS – Université de Strasbourg

23 rue du Loess, BP 43

67034 Strasbourg Cedex 2

Abstract:

Polydopamine (PDA) deposition, obtained from the oxidation of dopamine and other catecholamines is an universal way to coat all known materials with a conformal coating which can subsequently be functionalyzed at will. The structural analogies between polydopamine and eumelanin, the black-brown pigment of the skin, incited to produce stable polydopamine nanoparticles in solution instead of amorphous precipitates obtained from the oxidation of dopamine. Herein, we demonstrate that size controlled and colloidally stable PDA based nanoparticles can be obtained in acidic conditions, where spontaneous auto-oxidation of dopamine is suppressed, using sodium periodate as the oxidant and a protein like alkaline phosphatase as a templating agent. The size of the PDA@Alp nanoparticles depends on the dopamine/enzyme ratio and the obtained particles display the enzymatic activity of alkaline phosphatase with an activity extending up to two weeks after particle synthesis. The PDA@ alkaline phosphatase (Alp) nanoparticles can be engineered in polyelectrolyte multilayered films to potentially design model biosensors.

Keywords: melanin like nanoparticles, sodium periodate, enzymatic activity, layer-by-layer films.

Introduction.

Inspired by the adhesion of mussels [1] to the surface of wood or stones in a wet environment, dopamine [2] and other catecholamines [3, 4] were proven to be interesting molecules to coat the surface of all known materials with a conformal coating having an adjustable thickness from a few nm to more than 100 nm. The oxidation of dopamine and its subsequent self-assembly/polymerization [5,6] is at the origin of the deposition of those "polydopamine" (PDA) films on various substrates. In the presence of Tris buffer at pH = 8.5, the film thickness saturates at 40-45 nm after about 16 h of auto-oxidation in the presence of dopamine at 2 $mg.mL^{-1}$ [2]. Thicker but also rougher films can be obtained by further increasing the dopamine concentration in otherwise identical conditions [7]. A major drawback of PDA and related films is the slow deposition kinetics. This problem was addressed and partially solved by depositing PDA by means of spray deposition [8] or using stronger oxidants than the oxygen dissolved in water [9-11].

The resulting PDA films, can be deposited at all interfaces, even at water/air interfaces [12] to get flexible and asymmetric membranes in the presence of polyamines [13] or catechol bearing polymers [14] in the aqueous subphase. In all cases however, the deposition of conformal PDA films is accompanied by the precipitation of an amorphous and useless precipitate.

Inspired by the structural analogies between PDA and eumelanins [15,16], the black-brown pigment of the skin and dark hairs, and the homogeneous-hierarchical size distribution of the eumelanin grains of the skin or sepia ink [17], attempts were made to produce colloidally stable PDA nanoparticles in solution. On the one hand, synthesis in the presence of ethanol/water mixtures and using ammonia as a catalyst allows to produce PDA of controlled size in the 100 nm range [18, 19] with numerous applications in cancer therapy owing to the photothermal effect afforded by the optical properties of PDA [20] and in biosensing [21]. Some polymers like poly(vinyl alcohol) [22] and surfactant micelles [23] allow to produce stable suspensions of PDA. Of major interest is to notice that eumelanin grains are always surrounded by a tightly bound protein layer [24], making the purification of eumelanins a difficult task. Melanosomal proteins, the organelle where eumelanin is synthesized, allow to increase the rate of eumelanin formation and associate with the obtained particles [25]. Therefore some successful attempts were made to synthezise PDA in the presence of proteins. In particular, human serum albumin

(HSA) was found to increase the rate of PDA formation and to allow for the formation of stable, biocompatible nanoparticles [26]. Tyrosine containing tripeptides allow also to control the formation of eumelanin particles in a sequence dependant manner [27]. In the case of HSA, the size of those nanoparticles was dependent on the initial protein/dopamine molar ratio and simultaneously to the formation of nanoparticles, the deposition of PDA films on the surface of the reaction beaker was progressively inhibited. Other proteins were found to play a similar role and the presence of a solvent accessible diad of two amino acids, namely L-Lysine and L-glutamic acid was found to play a crucial role in the formation of PDA nanoparticles [28]. However those nanoparticles were all produced at pH = 8.5 by oxygen triggered auto-oxidation of dopamine, a pretty slow reaction mechanism.

Herein, we are wondering if the templating role of proteins can be conserved in the presence of a strong oxidant like sodium periodate which was shown to allow for the formation of PDA films about 100 nm in thickness in only two hours [11]. As a model protein, we choose alkaline phosphatase which was shown to allow to produce PDA rich-protein rich core–shell nanoparticles at pH=8.5 in the presence of dissolved oxygen [28].

Materials and Methods.

1.1.Chemicals and solutions

All chemicals were purchased and used without further purification. Dopamine-hydrochloride (ref. H8502), sodium periodate ($NaIO_4$, ref 311448), anhydrous sodium acetate (ref. W302406), para-nitrophenyl phosphate (PNP, ref. N7653), alkaline phosphatase from bovine intestinal mucosa (ALP, ref. P7640) were all from Sigma Aldrich. Tris hydroxymethyl aminomethane (Tris) was from Euromedex. All solutions were made from ultra-pure water (Milli Plus, Millipore, Billerica, MA USA). Dialysis tubings with a molecular weight cut off at 300 kDa were purchased from Spectrum Labs.

Two buffers were used: sodium acetate buffer at 50mM at pH 5.0 and Tris 50mM at pH 8.5. The pH of each buffer was adjusted with concentrated hydrochloric acid and checked with an Hannah 802 pH meter, calibrated in the pH range between 4.0 and 7.0 or 7.0 and 9.0 for the sodium acetate and Tris buffer respectively.

The diluted PNP solutions (from 5x to 100x) were solubilized in Tris buffer. The $NaIO_4$ (at 20mM) and the dopamine solutions were freshly prepared before each experiment in sodium acetate buffer.

1.2. Synthesis and characterization of polydopamine nanoparticles

Alkaline phosphatase (ALP) was first dissolved in sodium acetate buffer without any stirring. Then, dopamine at 2mg.mL^{-1} (10.6 mM) was added under continuous stirring. Directly after that, a small amount of $NaIO_4$ solution was added, always under continuous stirring, and that during 6 hours at ambient temperature (17-20°C). The final concentration of oxidant was 20 mM in all experiments whereas the ALP concentration was changed from 0 (reference experiment) to 4 mg.mL^{-1}.

After synthesis, the solution was put in a dialysis tubing and dialyzed against Tris buffer for 24h approximatively, and with 3 buffer changes. At the end, the solution of PDA particles is stored at 4°C in a glass beaker or immediately used for characterization experiments. The particles obtained in the presence of ALP will be called PDA@ALP in the following.

The colloidal stability of the nanoparticles was investigated as a function of their storage time at 4°C, after dialysis with a NanoZS device (Malvern) to measure their electrophoretic mobility. The electrophoretic mobility was subsequently converted in a zeta potential value using the Smoluchowski approximation. This approximation is justified a posteriori for nanoparticles with a diameter larger than 30 nm in the sodium acetate buffer having an ionic strength of 32 mM at pH = 5.0.

For Cryo-TEM characterization, a drop of the dialyzed PDA@ALP solution was deposited on an electron microscopy grid covered by a hydrophobic carbon membrane. The drop size was progressively reduced in order to obtain a thin film covering the whole membrane. The grid was subsequently plunged into ethane at liquid nitrogen temperature. By maintaining the specimen at this temperature, the grid was transferred on the cryo-holder and inserted in the column of the electron microscope. These grids were analysed with a JEOL 2100F (S)TEM microscope working at 200 kV and equipped by a probe aberration corrector, an EELS (Gatan Tridiem) spectrometer and an EDX (Si-Li) detector. This set-up allows to reach resolutions of 2 Å and 1.1 Å under TEM and STEM modes, respectively. For limiting the irradiation damage, the images were acquired by using a low density of the electron beam.

1.3. Enzymatic activity of the PDA@ALP nanoparticles

The enzymatic activity of the solutions containing the PDA@ALP nanoparticles was measured by following the production of paranitrophenol from the hydrolysis of

paranitrophenol phosphate (PNP). The mother solution of PNP had a concentration of (4.6 ± 0.4)x 10^{-4} mol.L^{-1} as determined using a method described elsewhere [30]. To determine the activity of the particles, the absorbance of solutions containing PNP and PDA@ALP mixtures was measured with a double beam mc² UV Vis spectrophotometer (SAFAS, Monaco) at a wavelength of 405nm, taking an absorbance measurement every 10 seconds. The reference cuvette contained a mixture of PNP (3mL) and Tris (1mL) to account for the spontaneous hydrolysis of PNP. The studied solution was prepared with 3mL of PNP and 1mL of nanoparticles (1mL of buffer in the reference cuvette). The influence of both the substrate concentration and the dilution of the nanoparticles were investigated. The kinetic experiments covered a period of 15 min. For investigating the evolution of the enzymatic activity with storage time, the suspension of nanoparticles was stored at 4°C between two successive measurements. As control experiment, the activity of ALP in the presence of $NaIO_4$, a strong oxidant able, to oxidize amino acid close to the active center of the enzyme, was investigated. An exponential decrease law was fitted to the experimental kinetics as expected for a reaction of pseudo first order with respect to the substrate:

$$A_{405nm}(t) = A_{max}.(1 - e^{-k.t}) \quad (1)$$

,where A_{max} and k are the maximal measured absorbance (corresponding to consumption of all the substrate) and the rate constant respectively.

1.4 Layer-by-layer deposition of the PDA@ALP nanoparticles and enzymatic activity in the immobilized state.

The negatively charged (as inferred from zeta potential measurements) PDA@ALP nanoparticles obtained in the presence of ALP at 1 mg.mL^{-1} after 6h of dopamine oxidation and intensive dialysis against Tris buffer were used to deposit polyelectrolyte multilayer films [30, 31] in alternance with poly(allylamine) at 1 mg.mL^{-1} in the same buffer as a polycation. The films were deposited on plasma cleaned quartz slides (4 cm x 1 cm) using a deposition time of 5 min per deposition step and subsequent rinsing with 50 mM Tris buffer. The absorption spectrum of the dried films was measured with an mc² spectrophotometer every two layer pairs using a cleaned quartz slide as the reference, to follow the regular deposition of PDA@ALP nanoparticles and of PAH. The film deposition always started with the adsorption of the polycation PAH owing to the negative charge of the quartz substrate under these conditions. The morphology of the $(PAH\text{-}PDA@ALP)_6$ films was investigated in the dry state by contact

mode AFM (Nanoscopoe III, Bruker), using an MLCT-C cantilever (nominal spring constant: 0.01 $N.m^{-1}$). The enzymatic activity of the films was estimated as a function of the number of (PAH-PDA@ALP) layer pairs by immersing the films in 3 mL of 20 fold diluted PNP solutions. The reference cuvette contained the same PNP solution in Tris buffer at pH = 8.5 to compensate for the spontaneous hydrolysis of PNP.

Results and discussion

The dopamine solution was initially transparent at pH = 5.0 for which the oxygen triggered auto-oxidation is an extremely slow process. After addition of the oxidant, $NaIO_4$, either in the absence or in the presence of ALP, the solution turned yellow instantaneously and then red which is characteristic of the formation of dopaminochrome [11] and finally black after 4 hours of oxidation.

From a more quantitative point of view, we investigated the kinetics of the formation of nanoparticles in the presence and in the absence of ALP by UV vis spectroscopy. An illustrative experiment is displayed in Figure 1, where it appears that ALP present at a concentration of 0.5 or 1 $mg.mL^{-1}$ is able to produce PDA aggregates faster than in the absence of the enzyme from a 2 $mg.mL^{-1}$ dopamine solution compared to the reference case in the absence of enzyme. These results are similar to those obtained for dopamine in the presence of ALP but at pH = 8.5 in the absence of another added oxidant [28]. This increase in the oxidation rate of dopamine in the presence of ALP is also similar to the influence found for HSA but at pH = 8.5 in the presence of dissolved oxygen as the oxidant [26].

Preprints (www.preprints.org) | NOT PEER-REVIEWED | Posted: 29 September 2018 doi:10.20944/preprints201809.0575.v1

Peer-reviewed version available at Biomimetics 2018, 3, 36; doi:10.3390/biomimetics3040036

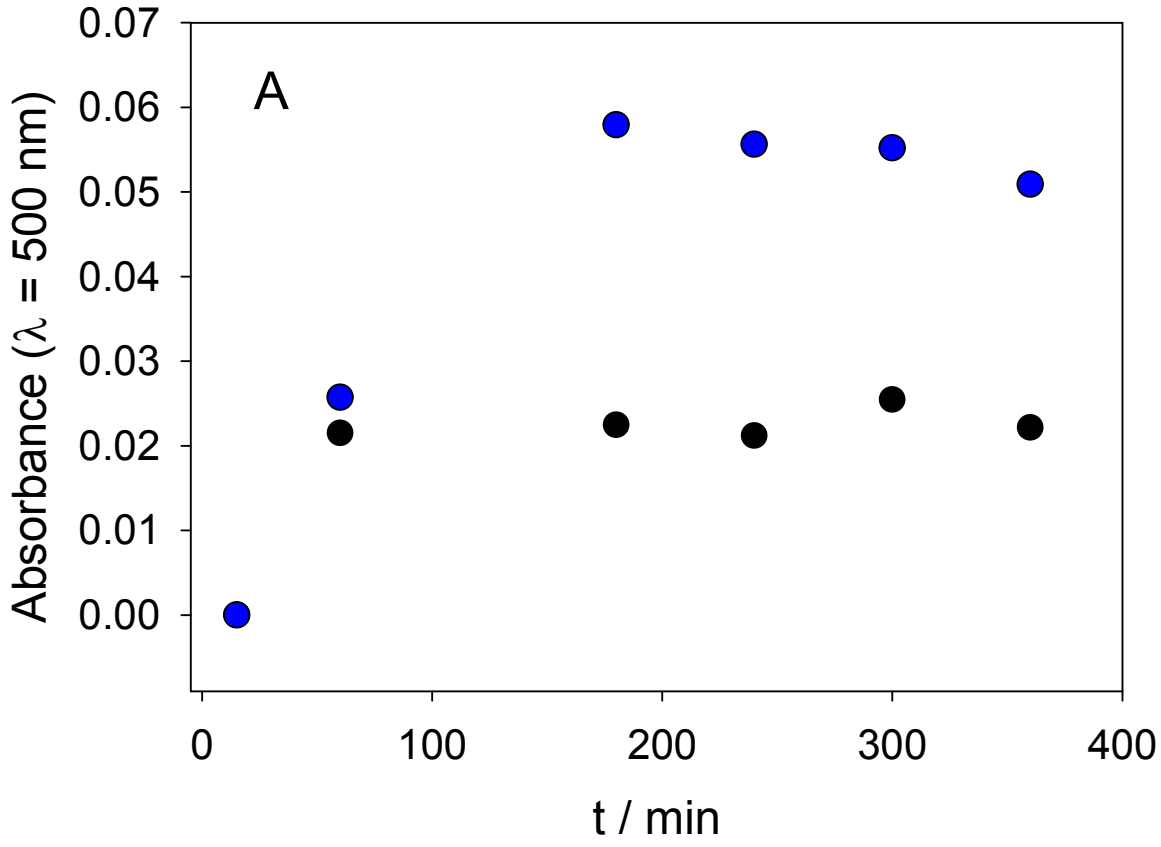

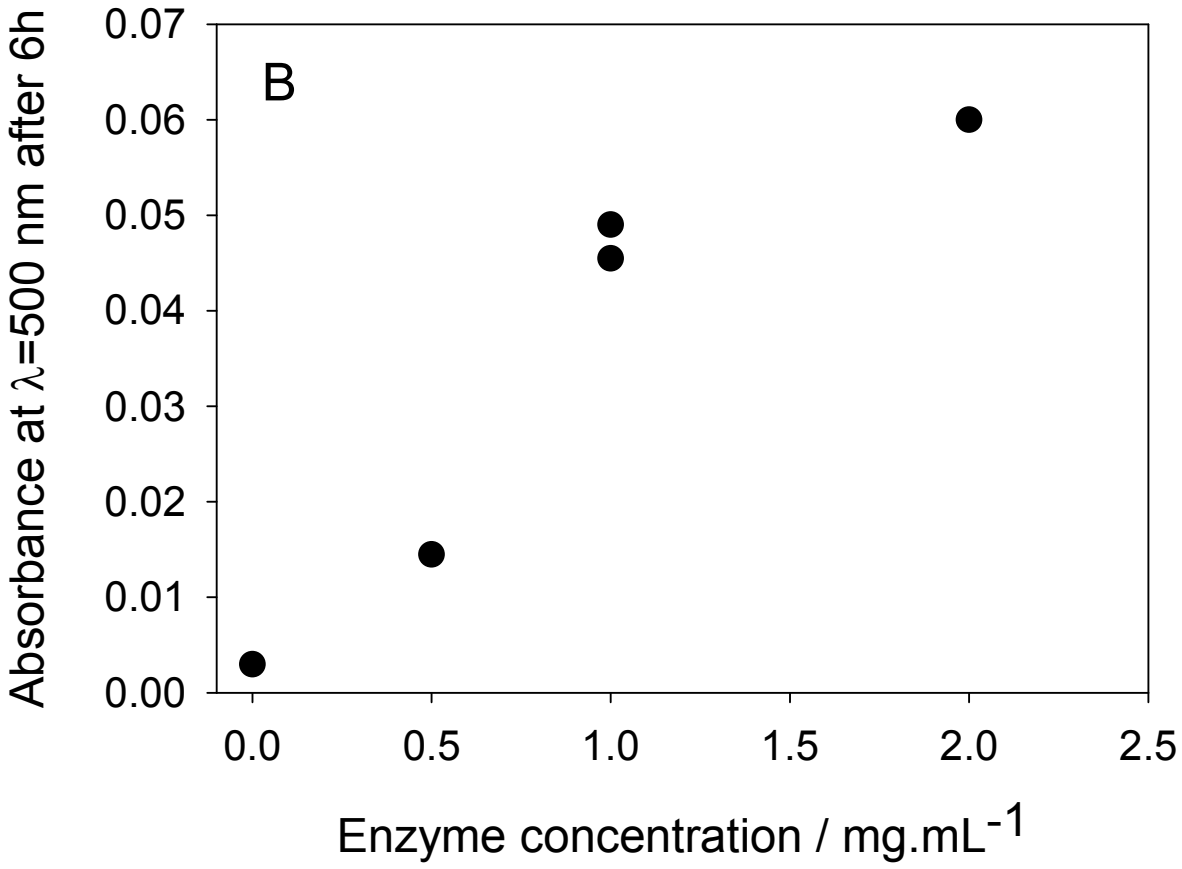

Figure 1: A: Evolution of the absorbance at 500 nm at pH = 5.0 in the presence of 20 mM $NaIO_4$ in the absence of enzyme (●) and in the presence of ALP at 1 $mg.mL^{-1}$ (●). The initial dopamine concentration was equal to 2 $mg.mL^{-1}$ in all cases.

B: Evolution of the absorbance after 6 h of dopamine oxidation (2 $mg.mL^{-1}$ at pH = 5.0) as a function of the concentration of initially added ALP.

As an interesting finding, the absorbance reaches a saturation value after only a few hours of oxidation in the presence of $NaIO_4$ whereas the process is much slower at pH = 8.5 using dissolved oxygen as the oxidant [26, 28]. This result is in line with the fast formation of PDA films using $NaIO_4$ as the oxidant [11].

The size of the nanoparticles obtained after 6h of oxidation and subsequent dialysis of the reaction medium was obtained by TEM analysis (Figure 2). It appears clearly that an increase in protein concentration induces a significant reduction in the average size of the PDA nanoparticles.

In the presence of 20 mM $NaIO_4$ as oxidant, the effect of the enzyme is however less pronounced than in the case of PDA synthesized at pH = 8.5 using dissolved O_2 as the oxidant. In this later case the average particle size was reduced from about 500 to 50 nm when the ALP concentration was increased from 0 to 2 $mg.mL^{-1}$ [28] The fact that the PDA particles are smaller when synthesized in the presence of $NaIO_4$ versus O_2 may well originate from the fact that $NaIO_4$ not only allows to produce 5,6indolequinone in a single chemical pathway but may also degrade the obtained polydopamine [11].

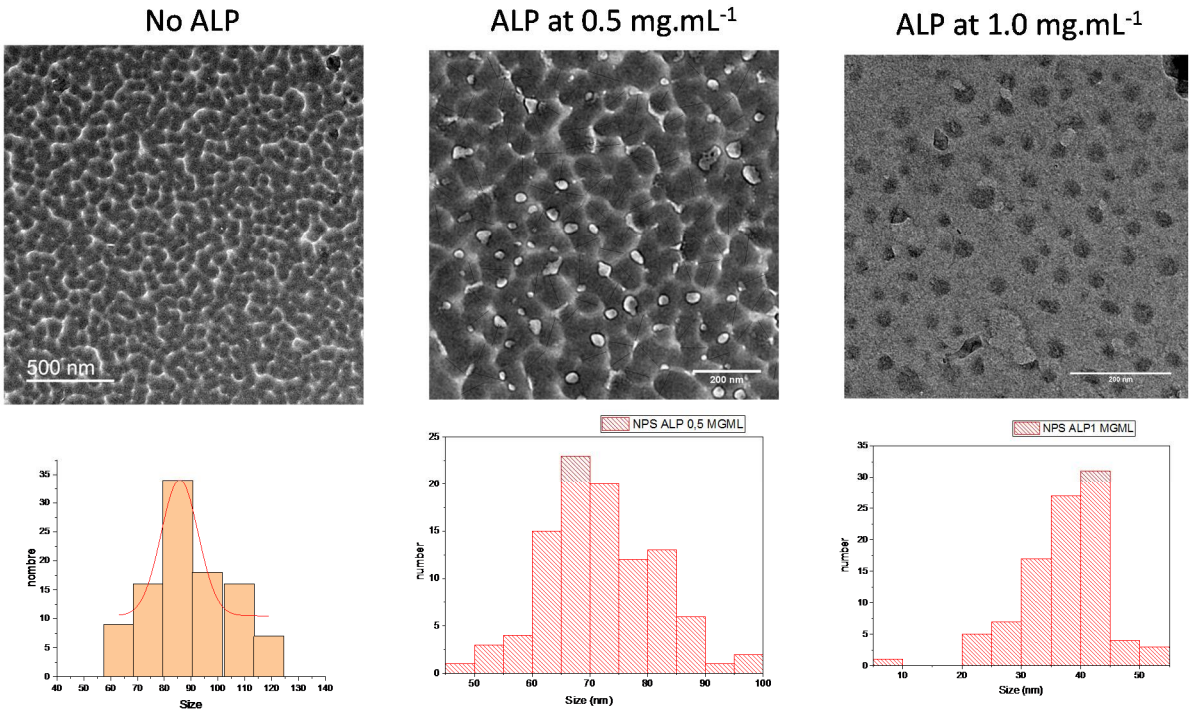

Figure 2: Top: Representative TEM micrographs of the PDA nanoparticles produced after 6 h of oxidation in the presence of 20 mM $NaIO_4$ from the dopamine solutions (10. 6 mM) after the subsequent dialysis against Tris buffer, as a function of the added concentration in ALP.

Bottom: Size distribution of the particles obtained by analysing 100 particles.

TEM micrographs obtained at higher resolution show the presence of an external corona less dense than the core of the particles, suggesting that the composition of the external part of the particles is richer in protein than the core (Figure 3).

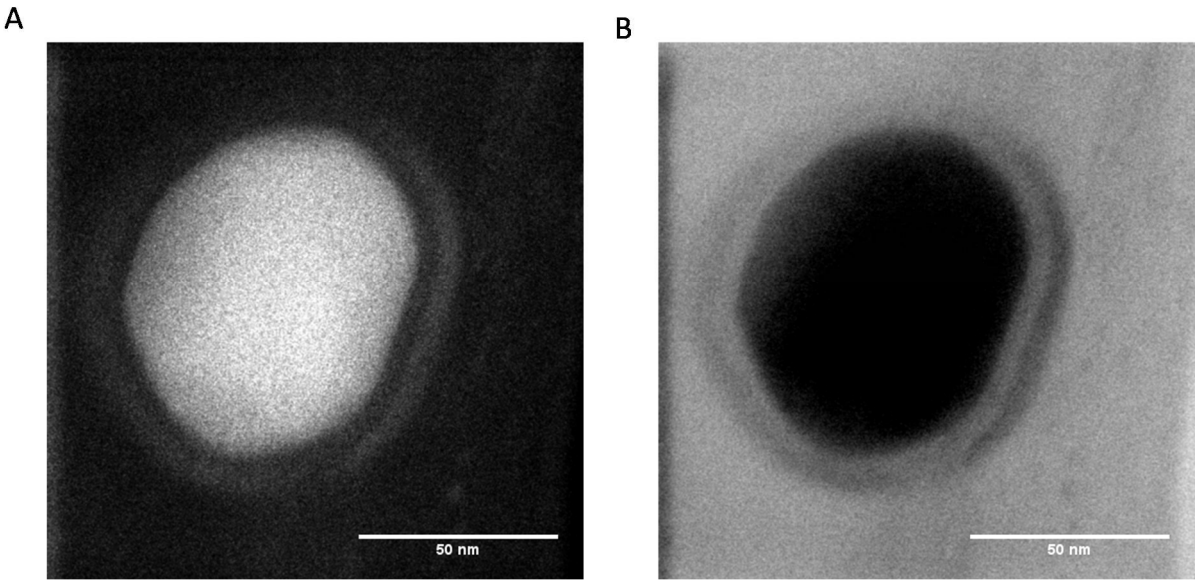

Figure 3: High resolution S-TEM images acquired simultaneously in high angle annular dark field (HAADF) and bright field (BF) modes of PDA@ALP nanoparticles obtained after 6 h of oxidation of a 10 mM dopamine solution + 1 $mg.mL^{-1}$ ALP in the presence of 20 mM $NaIO_4$.

Nevertheless at the present stage of our investigation we do not have a definitive proof that the obtained PDA@ALP nanoparticles are of the core shell type. It seems just that the corona of the particles may be richer in protein than the core. But owing the preparation method of the nanoparticles, just by mixing dopamine and the enzyme, we cannot exclude that proteins are also present in the core of the particles.

Anyway it appears that oxidation of dopamine in the presence of ALP in acidic conditions and using $NaIO_4$ as the oxidant allows to produce small nanoparticles in a much faster way then at pH = 8.5 under auto-oxidation conditions. This is a major advantage provided that the obtained nanoparticles are stable and are of use for biological applications. Indeed, the obtained PDA@ALP nanoparticles were stable from a colloidal point of view with no sedimentation during weeks as observed visually and a stable zeta potential during storage time (Figure 4). In addition, the zeta potential of the PDA@ALP nanoparticles was markedly different from the zeta potential of the large nanoparticles obtained in the absence of enzyme.

Peer-reviewed version available at Biomimetics 2018, 3, 36; doi:10.3390/biomimetics3040036

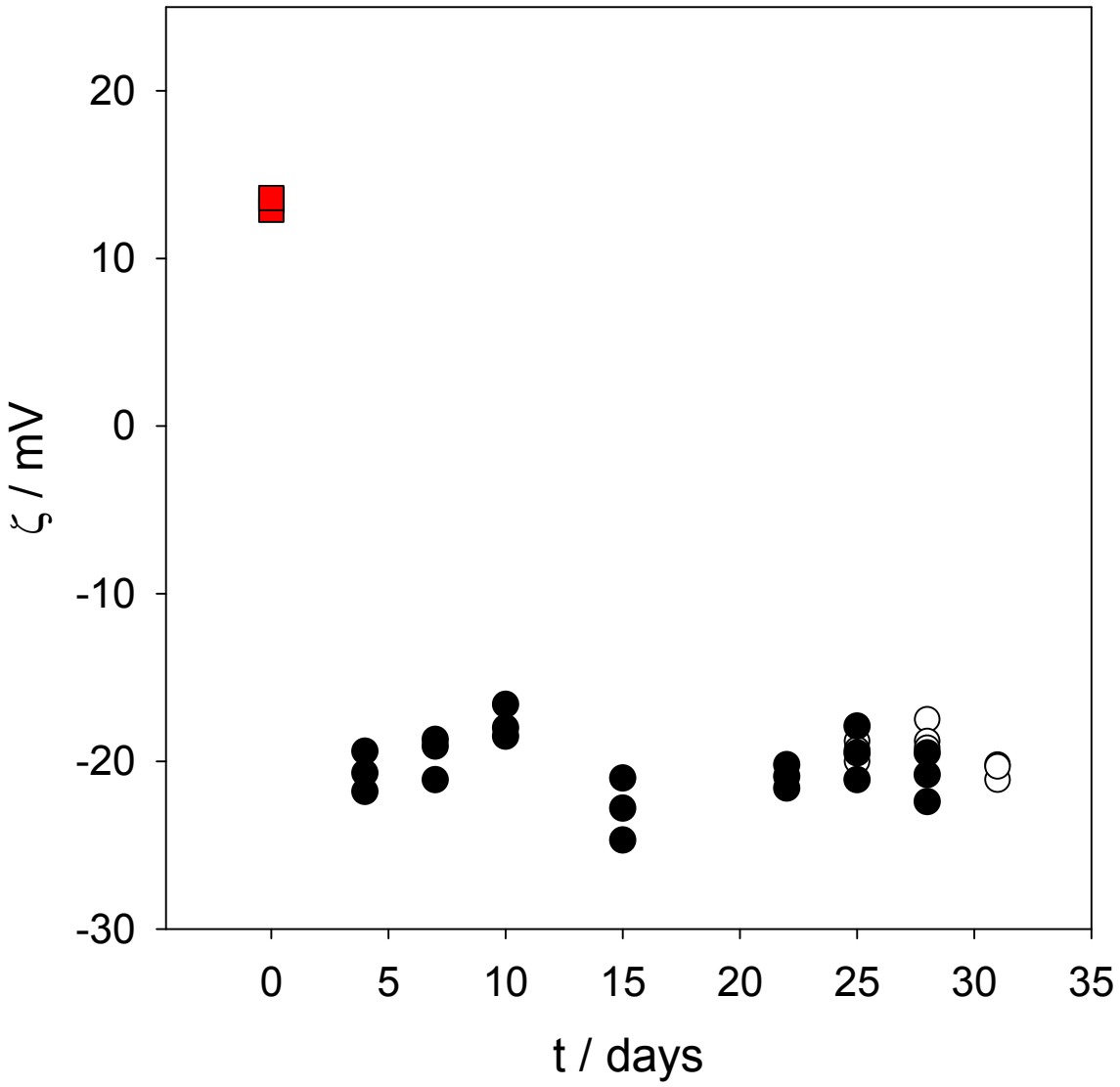

Figure 4: Zeta potential of PDA particles obtained after 6 h of oxidation of a 2 mg.mL^{-1} dopamine solution in the presence of 20 mM $NaIO_4$ without added enzyme (■) and in the presence of ALP at 1 mg.mL^{-1} (2 independent synthesis: ○,●). The particles suspension was dialyzed against Tris buffer as described in the Materials and Methods section. Each point corresponds to an individual measurement.

Even more interesting is the zeta potential reversal in the presence of ALP: pristine PDA displays a positive zeta potential at pH = 5.0 in agreement with the zeta potential of PDA films produced by auto-oxidation of dopamine (but at pH = 8.5), whereas the PDA@ALP displays a

negative zeta potential around -20 mV at pH = 5.0. This finding is in agreement with the observation that ALP is present in the corona of the obtained nanoparticles (Figure 3).

The possible presence of ALP on the surface of the PDA@ALP nanoparticles suggests to test if ALP keeps at least part of its enzymatic activity in these pretty harsh synthesis conditions. We first verified that ALP solubilized in 50 mM Tris buffer keeps its enzymatic activity when put in contact with 20 mM $NaIO_4$ (Figure 5).

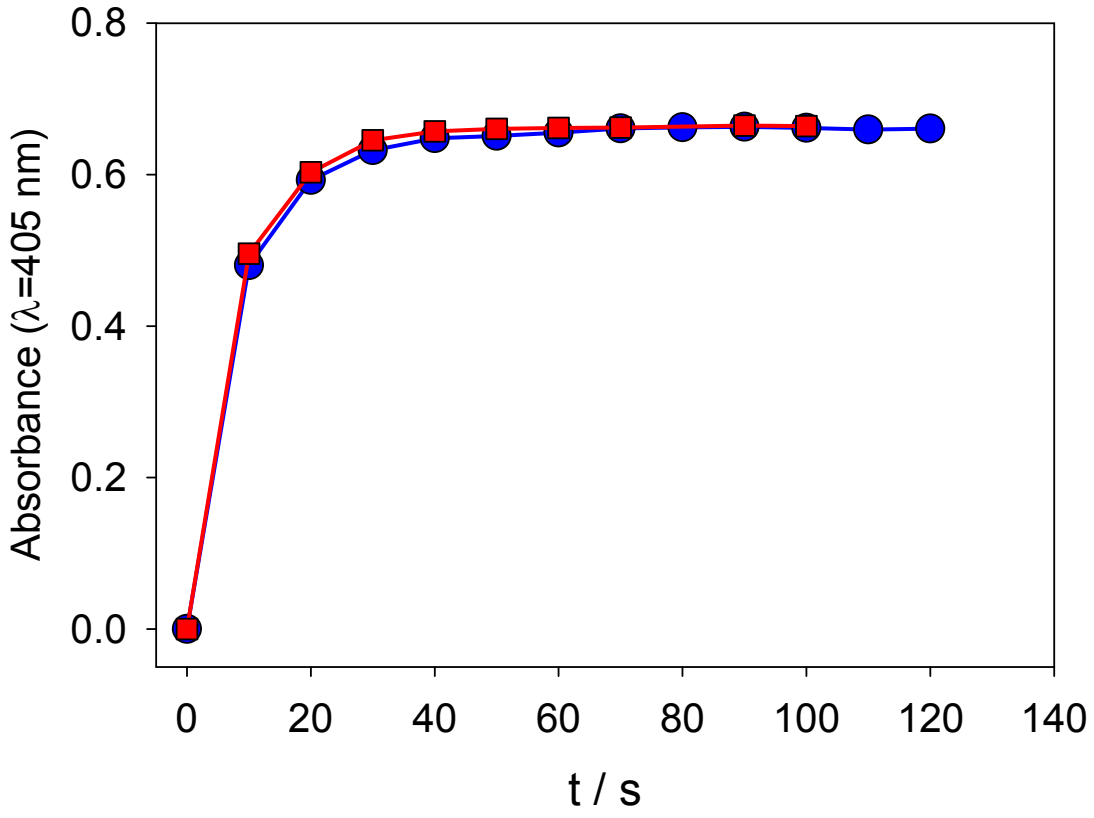

Figure 5: Enzymatic activity of ALP (0.1 $mg.mL^{-1}$) in the presence of 50 mM Tris buffer (—■—) and in the presence of 50 mM Tris buffer with 20 mM $NaIO_4$ (—●—).

The obtained findings strongly suggest that the strong oxidant does not affect the enzymatic activity of the enzyme itself, and this is reflected by the fact that the PDA@ALP particles keep the enzymatic activity expected for the enzyme after oxidative synthesis in the presence of $NaIO_4$ and subsequent dialysis against Tris buffer at pH = 8.5, i.e. the optimal pH for ALP. The obtained nanoparticles loose progressively their enzymatic activity upon storage at 4 °C (between two successive measurements) (Figure 6A). This loss in activity cannot be attributed to ALP desorption from the particle's surface, because we measured the activity of the particles in the presence of their supernatant buffer after appropriate dilution by a factor of 20. In

Preprints (www.preprints.org) | NOT PEER-REVIEWED | Posted: 29 September 2018 doi:10.20944/preprints201809.0575.v1

Peer-reviewed version available at Biomimetics 2018, 3, 36; doi:10.3390/biomimetics3040036

addition, this progressive loss in activity is reproducible on at least two independent particle batches (Figure 6B). It may represent a slow and progressive enzyme denaturation when grafted on the particles surface.

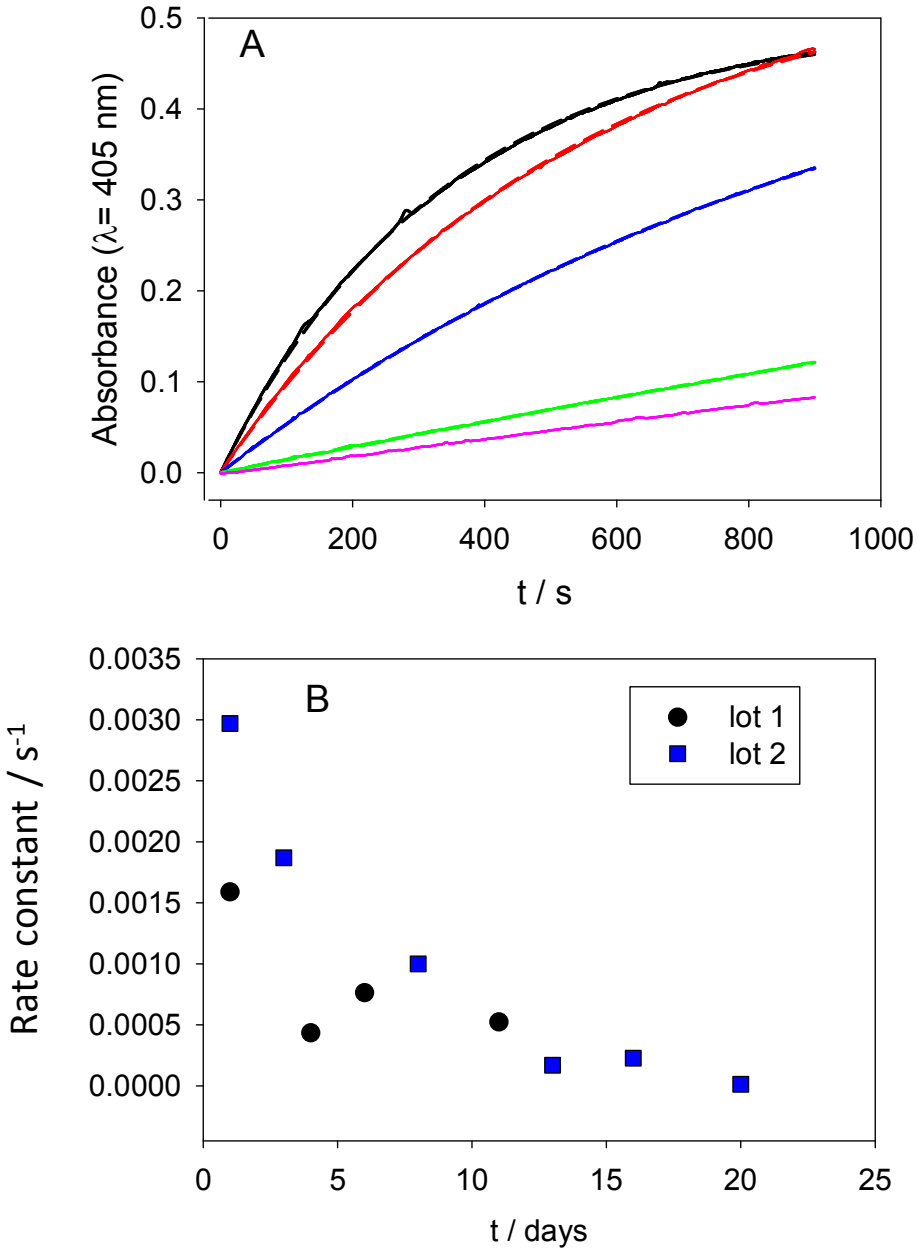

Figure 6:

A. Evolution of the enzymatic activity of a 10 fold diluted PDA@ALP nanoparticles suspension in the presence of a 20 fold diluted PNP solution at day 1 (____), 3 (____), 8 (____), 14 (____) and 20 (____) after the end of the particles dialysis step against Tris buffer at pH = 8.5.

B. Evolution of the rate constant of the enzymatic hydrolysis kinetics displayed in Figure6A for a first batch of particles (■: corresponding to the kinetics displayed in Figure 5A) and for an independent batch of particles (●).

Taking these results into account, we investigated the influence of both the nanoparticle relative concentration (expressed as the nanoparticle dilution in the following) and the substrate concentration on the enzymatic activity of PDA@ALP nanoparticles immediately at the end of the dialysis step against Tris buffer. The influence of the dilution in nanoparticles for a constant concentration in PNP (10 fold diluted mother solution, corresponding to an effective concentration of $(4.6 \pm 0.4)\text{x } 10^{-4}$ mol.L^{-1}) is given in Figure 7. The obtained linear relationship demonstrates that the PNP hydrolysis is a first order process with respect to the concentration in nanoparticles and hence also to the enzyme concentration available on the surface of the nanoparticles, as expected.

Preprints (www.preprints.org) | NOT PEER-REVIEWED | Posted: 29 September 2018 doi:10.20944/preprints201809.0575.v1

Peer-reviewed version available at Biomimetics 2018, 3, 36; doi:10.3390/biomimetics3040036

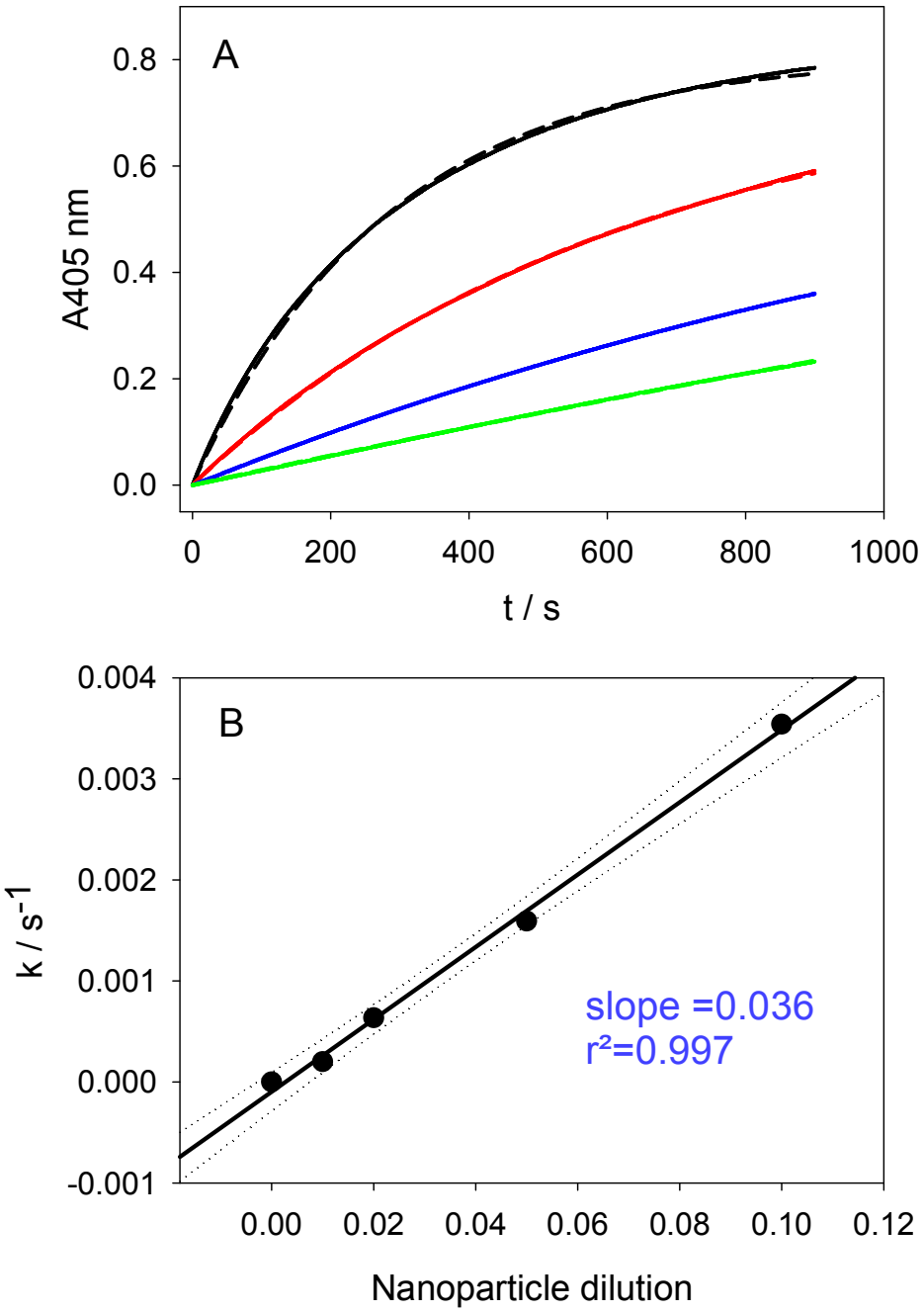

Figure 7:

A: hydrolysis of 10 fold diluted PNP solutions in the presence of PDA@ALP nanoparticles at different dilutions: mother suspension issued from the synthesis and dialysis diluted: 10 fold (____), 20 fold (____), 50 fold (____), 100 fold (____). The full lines correspond to the

experimental data whereas the dashed lines correspond to the fit of eq. (1) to the experimental data.

B: rate constant obtained by fitting eq. (1) to the experiments displayed in part A versus the nanoparticle dilution factor.

The same kinds of experiments were performed but changing the concentration of the substrate at a given concentration of the PDA@ALP nanoparticles. The results are displayed in Figure 8.

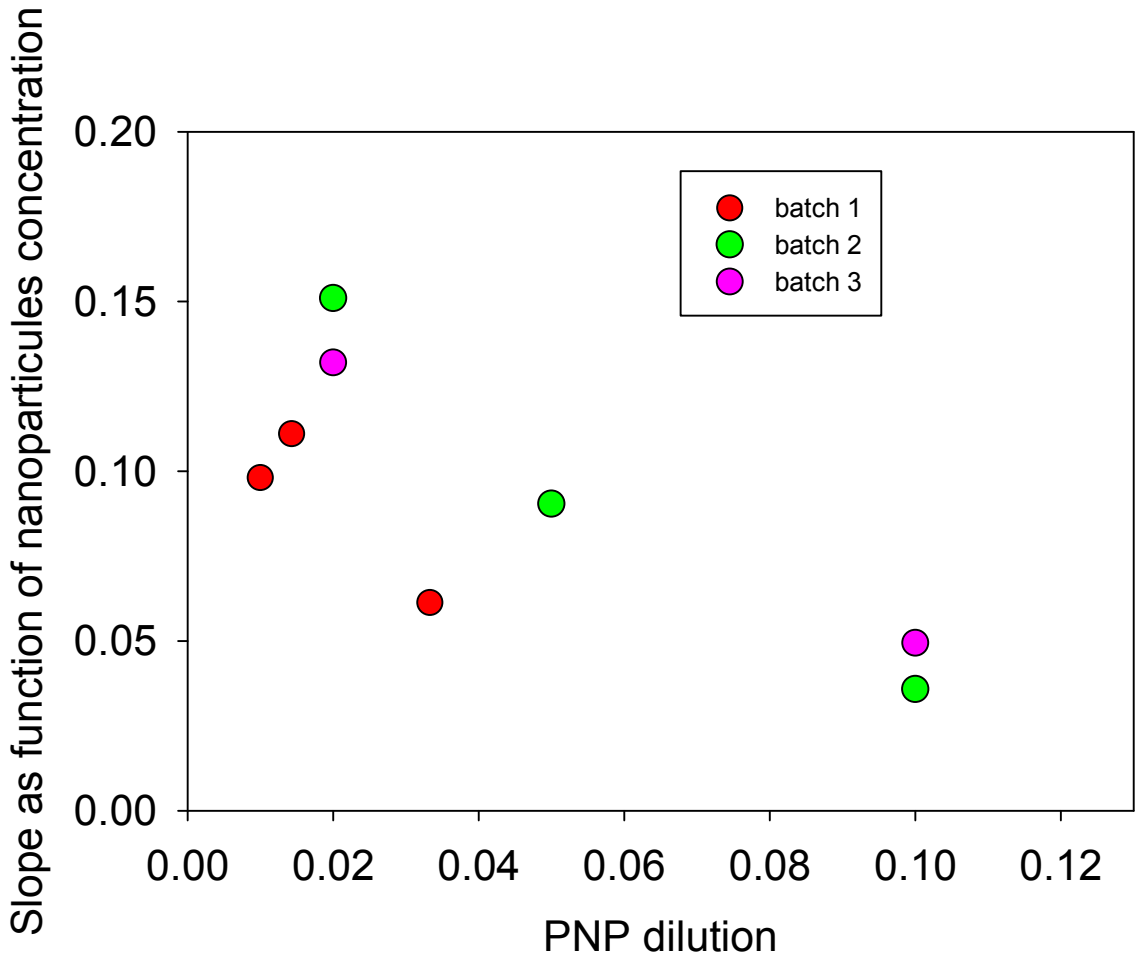

Figure 8: Evolution of the slope of the curves displayed in Figure 7B as a function of the PNP dilution (mother solution at $(4.6 \pm 0.4)\text{x } 10^{-4}$ mol.L^{-1}) for three independent batches of PDA@ALP nanoparticles.

For all the investigated particle batches, the rate constant for the hydrolysis of PNP decreases with the substrate concentration which proves that immobilized ALP on PDA nanoparticles is inhibited by its substrate.

Using the finding that the PDA@ALP nanoparticles keep the enzymatic activity of the grafted enzyme, we thought to use such particles as active components in thin films, which by using other more relevant enzymes, can be useful for the design of biosensors. Layer-by-layer deposited films [30, 31] offer the advantage to allow for a progressive increase in the surface concentration of active compounds owing to a regular growth process with the number of deposition steps. The $(PAH\text{-}PDA@ALP)_n$ films grow regularly with the number of deposition cycles *n* (Figure 9A) and the obtained films reflect the presence of nanoparticles close to about 100-400 nm in diameter as inferred by AFM imaging (Figure 9B) and as expected for films made from PDA@ALP nanoparticles prepared in the presence of ALP at 1 $mg.mL^{-1}$. This size is in relative agreement with the particles' size determined by TEM (Figure 2). In the immobilized state the particles may become closer than in solution and aggregate.

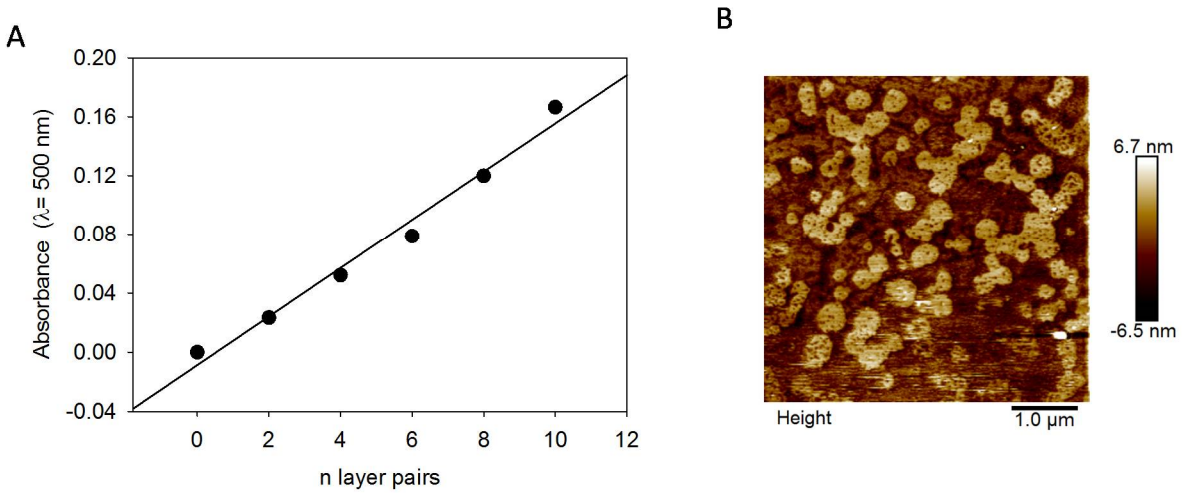

Figure 9: A: Evolution of the absorbance at λ = 500 nm (where PAH does not absorb light) of $(PAH\text{-}PDA\ @ALP)_n$ films with the number of deposited layer pairs, *n*.

B: Film morphology of a $(PAH\text{-}PDA@ALP)_6$ film as investigated by means of contact mode AFM.

The activity of the $(PAH\text{-}PDA@ALP)_n$ films was then measured as function of the number of deposited layer pairs, *n*, and some representative kinetics are given in Figure 10. For reaction times as short as 15 min and for very low enzyme amounts present in the films, contrarily to the experiments performed in bulk (see Figure 7), the kinetics are linear. Such a linear regime corresponds of course to the first part of an exponential curve. The slope of those straight lines represents the rate of PNP hydrolysis which was then plotted as a function of the number of layer pairs in Figure 11. It appears that the hydrolysis rate of PNP scales proportionally with *n*, namely with the film thickness (see Figure 9). This means that all enzymes on the PDA@ALP nanoparticles are accessible to the substrate.

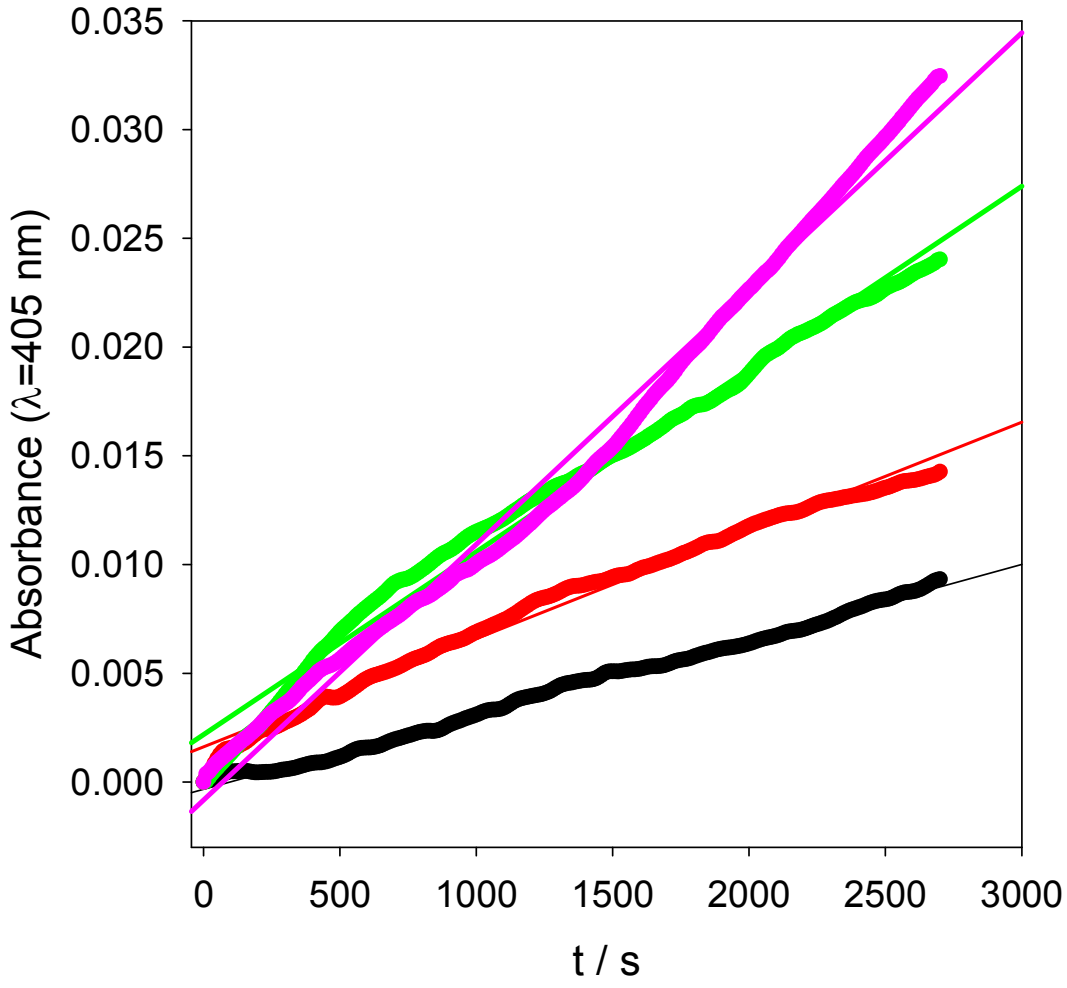

Figure 10: Enzymatic kinetics for (PAH-PDA@ALP)$_n$ films put in contact with a 20 fold diluted PNP solution as a function of the number of deposited layer pairs: n=3 (—●—), n=6 (—●—), n=12 (—●—) and n=15 (—●—). The points correspond to the experimental data whereas the full lines correspond to linear regressions to the data.

Preprints (www.preprints.org) | NOT PEER-REVIEWED | Posted: 29 September 2018 doi:10.20944/preprints201809.0575.v1

Peer-reviewed version available at Biomimetics 2018, 3, 36; doi:10.3390/biomimetics3040036

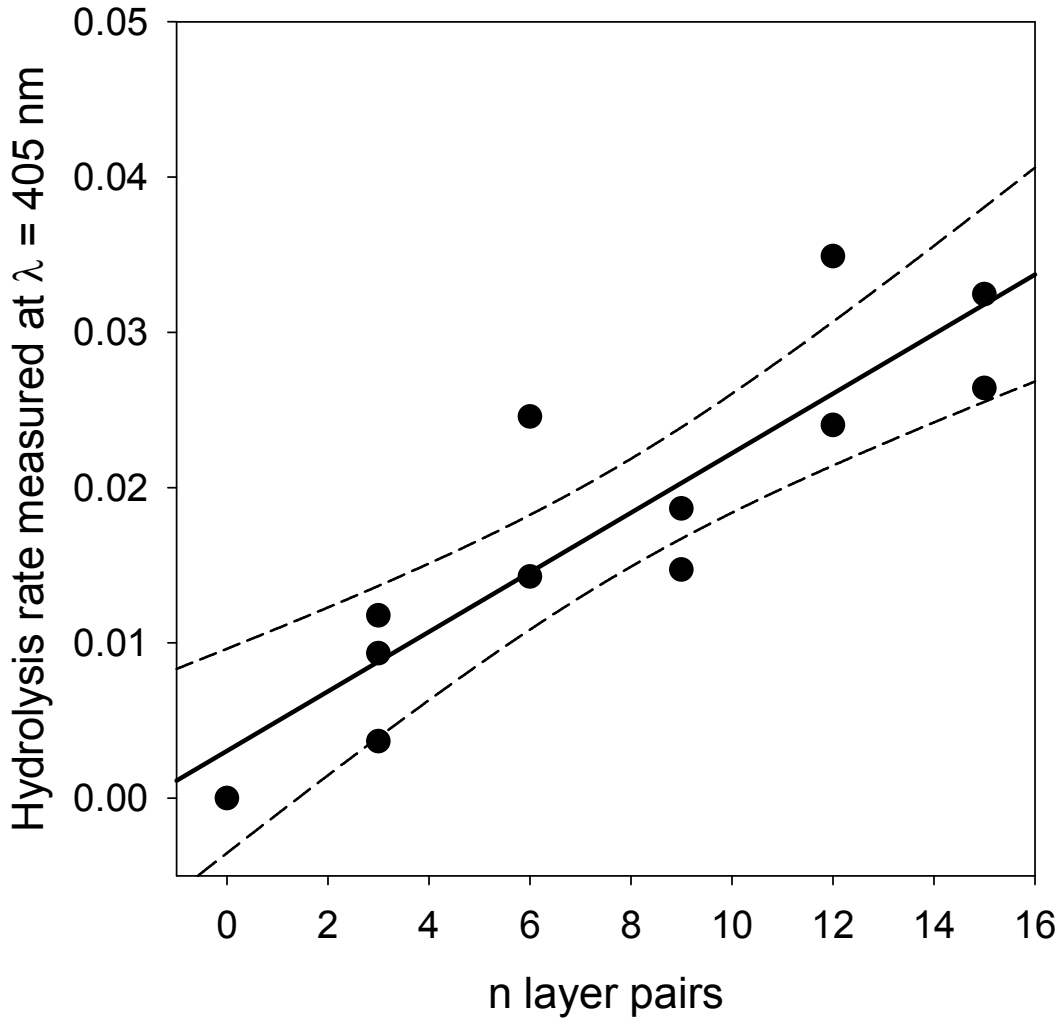

Figure 11: Evolution of the hydrolysis rate of $(PAH\text{-}PDA@ALP)_n$ films as a function of the number of deposited layer pairs. The full line corresponds to a linear regression to the data whereas the dashed lines correspond to the limit of the 95% confidence interval.

Conclusions

The oxidation of dopamine by $NaIO_4$ in the presence of alkaline phosphatase allows to produce stable nanoparticles of controlled size in a much shorter time than by auto-oxidation at pH = 8.5. Those nanoparticles keep the enzymatic activity of the used enzyme and seem to be enriched in enzyme on their corona with respect to their core. Owing to their negative charge, they can be immobilized in polyelectrolyte multilayer films with poly(allylamine

hydrochloride) to produce reactors with an activity proportional to the film thickness. The major challenge of this research remains to determine the accurate distribution of the enzyme in the nanoparticle to better understand the mechanism by which the enzyme controls the nanoparticle formation.

References.

[1] Lee B.P., Messersmith P.B., Israelachvili J.N. and Waite J.H. Mussel-inspired adhesives and coatings. *Ann. Rev. Mater. Res*. **2011**, 41, 99-132.

[2] Lee H., Dellatore S.M., Miller W.M. and Messersmith P.B. Mussel-inspired surface chemistry for multifunctional coatings. *Science*. **2007**, 318, 426-430.

[3] Kang S.M, Rho J., Choi, I.S., Messersmith P.B. and Lee H. Norepinephrine: material-independent, multifunctional surface modification reagent. *J. Am. Chem. Soc*. **2009**, *131*, 13224-13225.

[4] Hong S., Kim J., Na Y.S, Park J., Kim S., Singha K., Im G.-I., Han D.-K., Kim W.J. and Lee H. Poly(norepinephrine): ultrasmooth material-independent surface chemistry and nanodepot for nitric oxide. *Angew. Chem. Int. Ed*. **2013**, *52*, 9187-9191.

[5] Dreyer, D.R.; Miller, J.; Freeman, B.D. ; Paul, D.R.; Bielawski, B.W. Perspectives on poly(dopamine). *Chem. Sci*. **2013**, 4, 3797-3802.

[6] Liebscher, J.; Mrowczynki, R.; Scheidt, H.A.; Filip, C.; Hadade, N.D.; Turcu, R.; Bende, A.; Beck, S. Structure of polydopamine: a never-ending story ? *Langmuir 2013*, 29, 10539-10548.

[7] Ball V.; Del Frari, D.; Toniazzo, V.; Ruch, D. Kinetics of polydopamine film deposition as a function of pH and dopamine concentration: insights in the deposition mechanism. *J. Colloid Interf. Sci.* **2012**, *386*, 366-372.

[8] Schlaich C., Li M., Cheng C., Donskyi I.S., Yu L., Song G., Osorio E., Wei Q. and Haag R. Mussel-inspired polymer-based spray coating for surface modification: fast fabrication of antibacterial and superhydrophobic surface coatings. *Adv. Mater. Interf*. **2018**, Art 1701254.

[9] Wei Q., Zhang F., Li J., Li B. and Zhao C.Oxidant-induced dopamine polymerization for multifunctional coatings. *Polym. Chem*. **2010**, *1*, 1430-1433.

[10] Du X., Li L., Li J., Yang C., Frenkel N., Welle A., Heissler S., Nefedov. A., Grunze, M. and Levkin, P.A. UV-Triggered Dopamine Polymeization: Control of Polymerization, Surface Coating, and Photoppaterning. *Adv. Mater*. **2014**, *26*, 8029-8033.

[11] Ponzio, F.; Barthès, J.; Bour, J.; Michel, M.; Bertani, Ph.; Hemmerlé, J.; d'Ischia, M.; Ball, V. Oxidant control of polydopamine surface chemistry in acids: a mechanism based entry to superhydrophilic-superoleophobic coatings. *Chem. Mater*. **2016**, *28*, 4697-4705.

[12] Ponzio, F., Payamyar, P.; Schneider, A.; Winterhalter, M.; Bour, J., Addiego, F.; Krafft, M.-P.; Hemmerle, J.; Ball, V. Polydopamine films from the forgotten air/water interface. *J. Phys. Chem. Lett*. **2014**, *5*, 3436-3440.

[13] Hong S., Schaber C.F., Dening K., Appel E., Gorb S.N. and Lee H. (2014) Air/water interfacial formation of freestanding, stimuli responsive, self-healing catecholamine Janus faced microfilms. *Adv. Mater*. **2014**, *26*: 7581-7587.

[14] Ponzio, F.; Le Houerou, V.; Zafeiratos, S. ; Gauthier, C. ; Garnier, T. ; Jierry, L.; Ball, V. Robust alginate-catechol @polydopamine free standing membranes obtained from the water/air interface. *Langmuir* **2017**, *33*, 2420-2426.

[15] D'ischia, M.; Wakamatsu, K.; Napolitano, A.; Briganti, S.; Garcia-Borron, J-C.; Kovacs, D.; Meredith, P.; Pezzella, A.; Picardo, M.; Sarna, T.; Simon, J.D.; Ito, S. Melanin and melanogenesis: methods, standards, protocols. *Pig. Cell Melanoma Res*. **2013**, *26*, 616-633.

[16] d'Ischia, M.; Napolitano A.; Ball, V; Chen, C.-T.and Buehler, M.J. Polydopamine and melanins: from structure-property relationships to a unified tailoring strategy. *Acc. Chem. Res*. **2014**, *47*, 3541-3550.

[17] Clancy, C.M.R.; Simon, J.D. Ultrastructural organization of eumelanin from Sepia Officinalis measured by atomic force microscopy. *Biochemistry* **1998**, *40*, 13353-13360.

[18] Liu, H.; Ai, K.; Liu, J.; Deng, M.; He, Y.; Lu L. Dopamin-melanin colloidal nanospheres: an efficient near-infrared photothermal therapeutic agent for in vivo cancer therapy. *Adv. Mater*. **2013** , 25 : 1353-1359.

[19] Wang, Z.; Wang, K.; Zhang, Y.; Jiang, Y.; Lu, X.; Fang, L.; Gan, D.; Lv, C.; Zhang, H. and Qu, S. Protein-affinitive polydopamine nanoparticles as an efficient surface modification strategy for versatile porous scaffolds enhancing tissue regeneration. *Particles & Part. Syst. Charac*. **2016**, 33, 89-100.

[20] Miao, Z.-H.; Wang, H.; Yang, H.; Li, Z.-L.; Zhen, L.; Xu, C.-Y. Intrinsically Mn^{2+}-chelated polydopamine nanoparticles for simultaneous magnetic resonance imaging and photothermal ablation of cancer cells. *ACS Appl. Mater. Interf*. **2015**, 7, 16946-16952.

[21] Qiang, W.; Li, W.; Li, X.; Chan, X.; Xu, D. Bioinspired polydopamine nanospheres: a superquencher for fluorescence sensing of biomolecules. *Chem. Sci*. **2014**, 5, 3018-3024.

[22] Arzillo, M.; Mangiapia, G.; Pezzella, A.; Heenan, R.K.; Radulescu, A.; Paduano, L.; d'Ischia M. Eumelanin buildup on the nanoscale: aggregate growth/assembly and visible absorption development in biomimetic 5,6-dihydroxyindole polymerization. *Biomacromolecules* **2012**, *13*, 2379-2390.

[23] Ponzio, F.; Bertani, Ph.; Ball, V. Role of surfactants in the control of dopamine-eumelanin particle size and in the inhibition of film deposition at solid-liquid interfaces. *J. Colloid Interf. Sci.* **2014**, *431*, 176-179.

[24] Guo, S.; Hong, L.; Akhremitchev; B.B.; Simon J.D. Surface elastic properties of human retinal pigment epithelium melanosomes. *Photochemistry & Photobiol*. **2008**, *84*. 671-678.

[25] Wagh S., Ramaiah R., Subramanian R.; Govindarayan R. Melanosomal proteins promote melanin polymerization. *Pig. Cell. Res.* **2000**, *13*, 442-448.

[26] Chassepot, A.; Ball, V. Human serum albumin and other proteins as templating agents for the synthesis of nanosized dopamine-eumelanin. *J. Colloid Interf. Sci.* **2014**, 414, 97-102.

[27] Lampel, A.; McPhee, S.A.; Park, H.-A.; Scott, G.C.; Humagain, S.; Hekstra, D.R.; Yoo, B.; Frederix P.W.J.M.; Li, T;-D.; Abzalimov, R.R.; Greenbaum, S.G.; Tuttle, T.; Hu, C.; Bettinger C.J.; Ulijn R.V. Polymeric peptide pigments with sequence-encoded properties. *Science* **2017**, 356, 1064-1068.

[28] Bergtold, C.; Hauser, D.; Chaumont, A.; El Yakhlifi, S.; Mateescu, M.; Meyer, F.; Metz-Boutigue, M.-H. ; Frisch, B. ; Schaaf, P.; Ihiawakrim, D.; Ersen, O.; Monnier, C.A.; Petri-Fink, A.; Rothen-Rutishauser, B.; Ball, V. Mimicking the chemistry of natural eumelanin synthesis: the KE sequence in polypeptides and in proteins allows for a specific control of nanosized functional polydopamine formation. Biomacromolecules .**2018**, 19, 3693-3704

[29] Ball, V. Activity of alkaline phosphatase adsorbed and grafted on polydopamine films. *J. Colloid Interf. Sci.* **2014**, 429, 1-7.

[30] Decher G. Fuzzy nanoassemblies: toward layered polymeric multicomposites. *Science* **1997**, 277, 1232-1237.

[31] Borges J.; Mano, J.F. Molecular interactions driving the layer-by-layer assembly of multilayers. *Chem. Rev.* **2014**, 114, 8883-8942.